PHILIPPINE ENGINEERING JOURNAL
PEJ 2022; Vol. 43, No. 2: 43-56

Received: 10 June 2022
Accepted: 23 October 2022

Effect of Electrostatic Interactions in the Separation of Magnetite and Silica using Enhanced Gravity Concentration

Karlo Leandro D. Baladad, Djoan Kate T. Tungpalan and Herman D. Mendoza
Department of Mining Metallurgical and Materials Engineering,
College of Engineering, University of the Philippines Diliman, Quezon City, Philippines

Abstract—*This study investigates the effect of electrostatic interactions in the separation of magnetite and silica in aqueous media using enhanced gravity concentration. As the effect of electrostatic interactions becomes more prominent in finer size ranges, understanding this correlation can help in determining what conditions will improve the performance of enhanced gravity concentrations. Magnetite and silica suspensions at different coagulation conditions were prepared and subjected to enhanced gravity concentration using a Falcon L40 concentrator. The resulting separations were then related to the observed coagulation responses.*

The zeta potential of magnetite as a function of pH and electrolyte concentration was measured using an electrophoretic method and the critical coagulation concentration of magnetite was determined using a UV-VIS Spectrometer. The total potential energy curves generated from the zeta potential and CCC data, showed the dominant forces that affect coagulation behavior at various pH levels. Repulsive forces were found to be most dominant at pH 11 for both magnetite-magnetite and magnetite-silica suspensions. Increased recovery of both magnetite and silica was observed at pH 3 where attractive forces are strongest both for one-component and two-component interactions. However, the increased recovery of both particles resulted in decreased separation efficiency at this condition. At pH 11, where repulsive forces are dominant for both one-component and two-component interactions, recovery of both particles decreased. The highest separation efficiency 64.1% was at pH 9. At this condition, magnetite-silica interactions were repulsive which led to the increased removal of silica. The attractive one-component interaction of the remaining magnetite particles led to its increased agglomeration and subsequently, increased magnetite recovery and grade at this condition.

Keywords: *Enhanced Gravity Concentration, Electrostatic Interactions, Falcon Concentrator, DLVO Theory, Zeta Potential*

I. INTRODUCTION

One of the oldest methods of concentrating valuable minerals is by gravity concentration. This concentration method has gained prominence due to its relative simplicity since it does not require any reagent or complex equipment. It also has minimal environmental impact compared to other concentration processes.[1] The decreasing grade of deposits, however, has also led to decreasing liberation sizes for valuable minerals. [2] Due to the limitations of traditional gravity concentration methods to process finer particles, enhanced gravity concentrators such as the Knelson Concentrator and the Falcon Gravity Concentrator have gained popularity[1][2][3][4] These equipment have effectively increased the size range wherein gravity concentration is applicable. Enhanced gravity concentrators involve a bowl rotating at very high speeds which exposes the feed material to centrifugal forces reaching up

to 300G's. The Falcon gravity concentrator can accommodate higher rotational speeds compared to the Knelson gravity concentrator. Meanwhile, the Knelson has more riffles which increase the available concentrating area in its bowl. [1][5]

This study focuses on the Falcon Gravity Concentrator which has a separation mechanism driven by the application of a centrifugal force that influences the stratification of particles within a liquid film in the inclined bowl of the concentrator. [6][7] Due to the angle of the wall in the stratification zone, as shown in Figure 1 and the high gravitational force generated by spinning, the slurry acts as a thin upward moving flowing film. [8][9] As the slurry moves upwards, the particles with higher densities develop high terminal velocities and adhere closely to the wall of the concentrate bowl. Eventually, these particles are retained in the retention zone where the concentrate will accumulate in a particle bed. On the other hand, lighter particles that are further from the wall experience a higher upward velocity from the flowing film of water allowing them to eventually exit the bowl. [8][9][10][11] The fluidization water which acts opposite to the centrifugal force can prevent the compaction of the particle bed, thus allowing the particles to be resuspended. This allows entrained light particles to report to the outer layer of the accumulated particle bed and gives them a greater chance to exit the retention zone and be caught in the upward flowing film.[12]

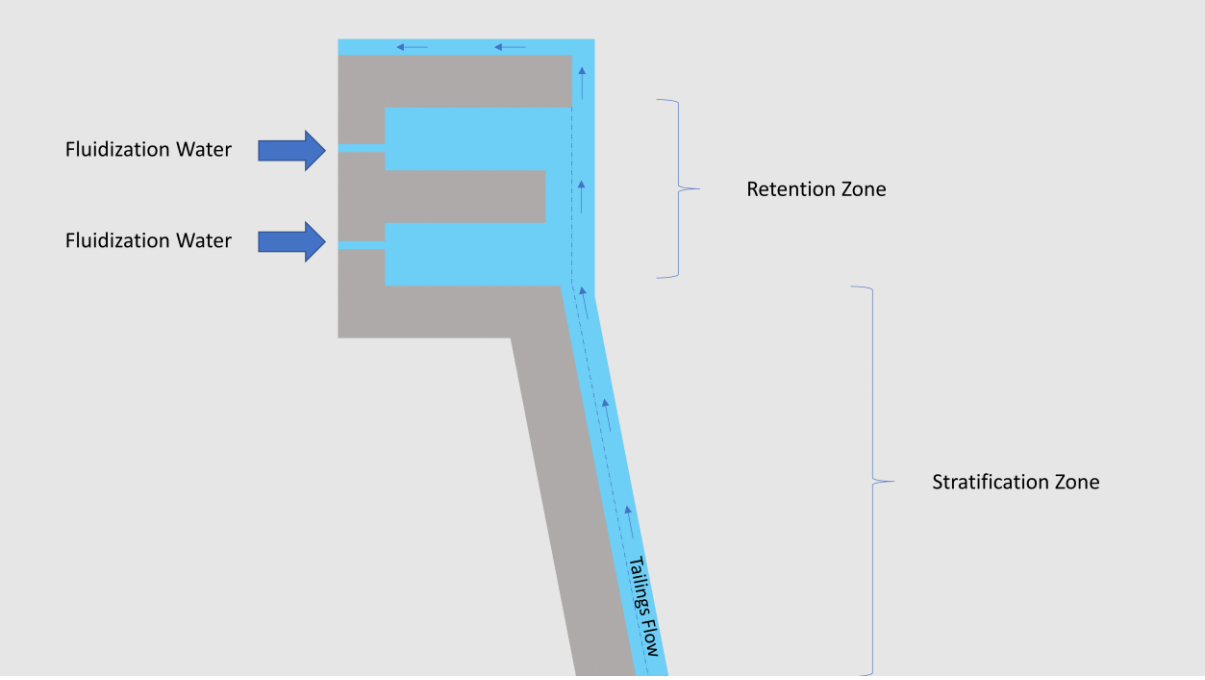

Figure 1. Schematic Diagram of L40 Falcon Gravity Concentrator

As particles sizes move to even finer size ranges, the effectivity of separation using enhanced gravity concentration still becomes increasingly difficult.[5][11][13] The decrease in performance is even more evident when concentrating minerals with lower specific gravity. [13][6] One possible way to address this issue is to study the electrostatic interactions of particles at fine size (<10μm) and how they affect particle agglomeration. Increased

agglomeration caused by electrostatic interactions could increase the settling rate and allow more particles to report closer to the wall of the concentrate bowl and be recovered. [14][15][16] Electrostatic interactions, however, can also cause repulsion to be the dominant force that affects particle interactions. When repulsive forces are more dominant, the terminal velocity of each individual particle is lower since agglomeration is less likely to occur. [14][17] This causes the particles to move as an uninterrupted suspension. This mode of transport allows particles to be more affected by currents such as the upward flowing film, which develops in the interface furthest from the wall of the bowl, thus, causing the particles to have a higher chance of exiting the concentrator and be included in the tailings.[18][19]

In this study, the effect of electrostatic interactions in the separation of magnetite and silica particles subjected to the Falcon concentrator was investigated. The interaction of magnetite and silica at different conditions were analyzed using Classical Derjaugin-Landau-Verwey-Overbeek (DLVO) theory. DLVO was used to predict whether attraction or repulsion will be the dominant particle interaction in the magnetite and silica suspensions. [20] Parameters such as recovery and separation efficiency were monitored and subsequently analyzed and put into context with the results of the DLVO analysis. The results of this study can help in understanding the conditions that can be used to increase the performance of enhanced gravity concentrations at lower size ranges.

II. MATERIALS AND METHODS

2.1 Mineral and reagents

The magnetite samples with particle size of less than 5 microns were of 99% purity, while the silica samples used were 1.5 microns and of 95% purity. The electrolyte used in all experiments was KNO_3. The pH of the suspensions was adjusted using 0.1 M HNO_3 and 0.1M KOH. For the zeta potential measurement and subsequent Falcon Concentration, the suspensions prepared were at pH 3, 5, 7, 9 and 11.

2.2 Zeta Potential Measurements

A Zeta Meter 2.0 was used for the zeta potential measurements. The suspensions prepared for the zeta potential measurements of both magnetite and silica had 50ppm solids concentration. The mobilities of at least 30 particles were tracked and the average mobility obtained was used to compute the zeta potential. The zeta potential data was used in the subsequent DLVO analysis of the magnetite and silica suspensions.

2.3 Critical Coagulation Concentration (CCC) Determination

To obtain the CCC, magnetite suspensions with varying electrolyte concentrations were prepared and then ultrasonicated at frequency of 53 KHz for 10 minutes to ensure that the particles were dispersed. The suspensions were adjusted to pH 11, with KOH used for pH adjustment, since it was at this condition that zeta potential of magnetite had the highest magnitude. 5µL samples were then obtained using a micropipette and were placed in a cuvette. The transmittance of the samples was determined using a Miniature Spectrometer, where the change in transmittance was tracked for 5 minutes for a duration of 30 minutes.

The transmittance values obtained were converted to turbidity using the equation:

$$\tau = -\left(\frac{1}{L}\right) \ln \%T \quad (1)$$

where τ is turbidity, L is the path length through the dispersion and T is the transmittance.[21]

The turbidity values after 30 minutes were plotted against electrolyte concentration. The steepest part of the graph was extrapolated to determine the point of inflection wherein an abrupt change in coagulation behavior occurs. [22] The CCC value will be used to compute the Hamaker constant of magnetite which will then be used to plot the total potential energy curves in the DLVO analysis.

2.4 Enhanced Gravity Concentration

For the Enhanced Gravity Concentration experiment, an L40 Falcon Concentrator was used (Figure 2). 200ml suspensions of magnetite and silica were prepared, with 3.0% solids by weight, to minimize the possibility of hindered settling.[1][23] Each suspension was also ultrasonicated at 53Khz for 180 seconds before it was subjected to the Falcon concentrator.

Equipment operational settings such as fluidization water pressure and rotational speed were kept at a constant value of 6psi and 200G, respectively.

After undergoing Falcon concentration, the concentrates obtained were dried for 2 hours. After drying, a niobium magnet was used to separate all the magnetite particles from the silica in the collected concentrate. The weight of the magnetite particles and silica particles were used to compute recovery and separation efficiency.

Figure 2. The L40 Falcon Gravity Concentrator used for concentration tests

2.5 Theoretical Considerations for DLVO Analysis

One important theory which adequately explains the inter-particle forces affecting particle stability is the Derjaguin–Landau–Verwey–Overbeek (DLVO) Theory.[24][25] It suggests that the stability of a colloidal suspension results from the sum of two forces: a repulsive force V_R due to the presence of an electrically-charged layer surrounding each particle, and an intermolecular force of attraction called the Van der Waals interaction, $V_{A.}$ [26][27]

As shown by the following equation, adding the Van der Waals attraction and the electrostatic repulsion gives the total potential energy between the particles:

$$V_T = V_A + V_R \tag{2}$$

For equal spherical particles, the electrostatic repulsion force V_R and the Van der Waals attraction V_A are respectively equivalent to the following equations [28][27]:

$$V_R \cong \frac{\varepsilon a_1 (\varphi_1{}^2)}{2} [\ln(1 + \exp(-\kappa H_o)] \tag{3}$$

$$V_A = - \frac{Aa}{12Ho} \tag{4}$$

For unequal spherical particles, the electrostatic repulsion force V_R and the Van der Waals attraction V_A are respectively equivalent to the following equations [28][27];

$$V_R \cong \frac{\varepsilon a_1 a_2 (\psi_1^2+\psi_2^2)}{4(a_1+a_2)} \left[\frac{2(\psi_1\psi_2)}{(\psi_1^2+\psi_2^2)} ln \frac{1+exp(-\kappa H_o)}{1-exp(-\kappa H_o)} + ln\{1 - exp(-2\kappa H_o)\}\right] \tag{5}$$

$$V_A \cong - \frac{A_{132} a_1 a_2}{6(a_1+a_2)H_o} \tag{6}$$

where ε is the dielectric constant of the solution, a is the radius of the particle in equation 3, a_1 and a_2 is the radii of dissimilar partictles in equation 4 and 5. Ψ is the surface charge, which is approximately equal to the zeta potential, κ is the Debye reciprocal length parameter, and Ho is the separation distance. A is the hamaker constant in equation 4 and A_{132} is the hamaker constant for particle 1 – water- particle 2 interaction in equation 6.

An important parameter in the calculation of the Van der Waals equation above is the Hamaker constant, A. To determine the Hamaker constant, the Critical Coagulation Concentration (CCC), wherein the electrostatic repulsion force is less than or equal to the Van der Waals interaction energy, must first be obtained. [26][29]

An experimentally determined value of the CCC and Hamaker constant of magnetite can make the calculation of the total potential energy more accurate.[26] The CCC for magnetite was determined by tracking the aggregation behavior of particles via changes in turbidity as mentioned in Section 2.4. [22][29]

The aggregation behavior of silica particles in aqueous solutions has been extensively studied. As summarized by Ackler et al., the Hamaker constant values for silica in aqueous solutions fall within 1.6×10^{-21} J-8.4×10^{-21} J. The Hamaker constant value for silica that was used in this experiment was 2.5×10^{-21} J as reported in the study made by Watillon et al. [30][31][32]

III. RESULTS AND DISCUSSION

3.1 DLVO Analysis

3.1.1 CCC and Hamaker Constant Determination

Figure 3 shows the turbidity values of the suspensions which were obtained every 5 minutes for a duration of 30 minutes. The data show that at higher concentrations, the suspension coagulates more rapidly. This is evidenced by the lower turbidity values at suspensions with higher concentration, indicating a greater degree of coagulation. The suspensions which have relatively lower concentrations of electrolyte (0.0001M, and 0.00001M KNO_3) remained significantly turbid even after 30 minutes. Increasing the concentration of the electrolyte resulted in faster aggregation and a less stable suspension. [26] [33][34]

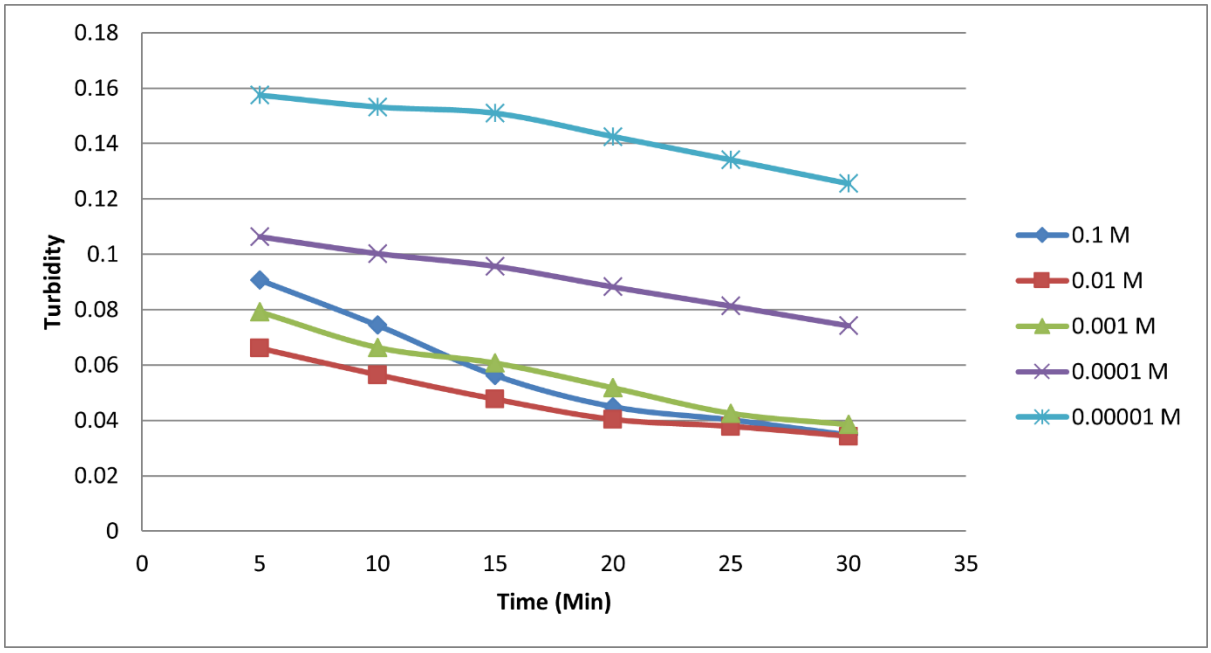

Figure 3. Turbidity of magnetite-magnetite suspension at different electrolyte concentrations of KNO_3 as a function of time

The CCC was obtained by plotting the turbidity values at the 30-minute mark with the corresponding electrolyte concentration as shown in Figure 4. Fast aggregation occurs at the region with higher concentrations, while slow aggregation occurs at the region with lower concentrations. Extrapolating the values and getting the intersection of the line of these two regions yielded a CCC value of 0.00105M, which was the value used to compute the Hamaker constant of magnetite. [22][29]

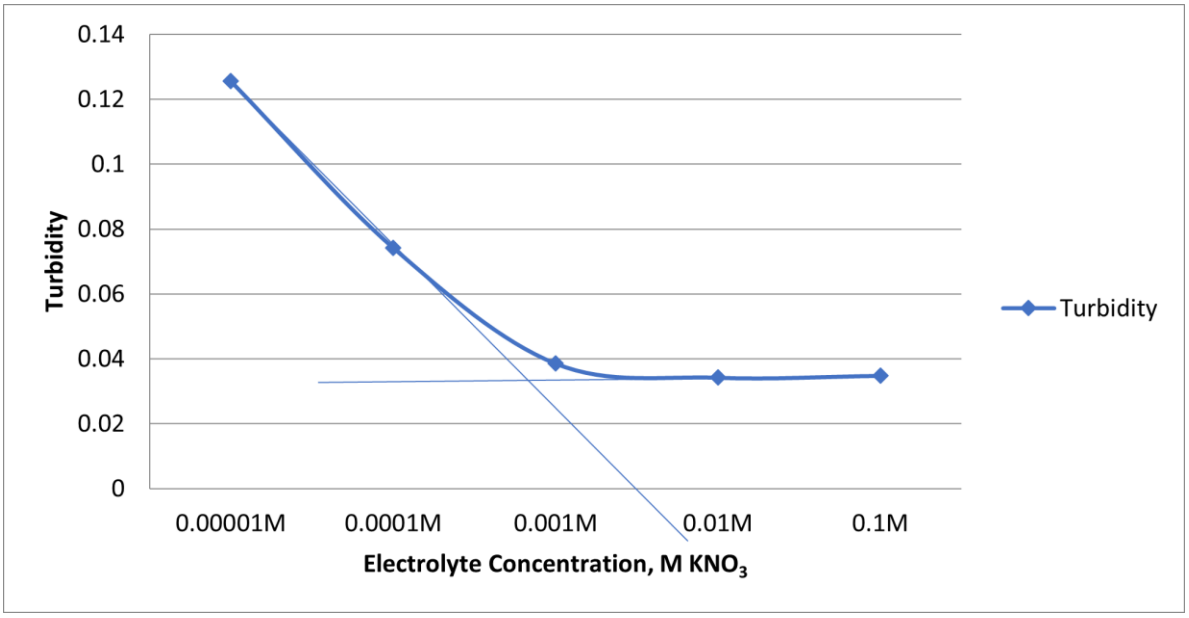

Figure 4. Turbidity of the suspension at different electrolyte concentrations of KNO_3

At the CCC, electrostatic repulsion V_R, and the Vander Waals attraction V_A, are equal. In this condition, there is no barrier to aggregation which allows for faster settling. [26][34] By using equations 2 and 3 and the zeta potential values in Figure 5, the Hamaker constant A was determined to be 2.22×10^{-20} J for magnetite. This value is within range of the Hamaker constants ($1\text{-}10 \times 10^{-20}$J) for magnetic substances (as summarized by Hu et al.). [26] The value is also close to the Hamaker constant obtained by Bergstrom et al. and Liu et al.[33] [35]

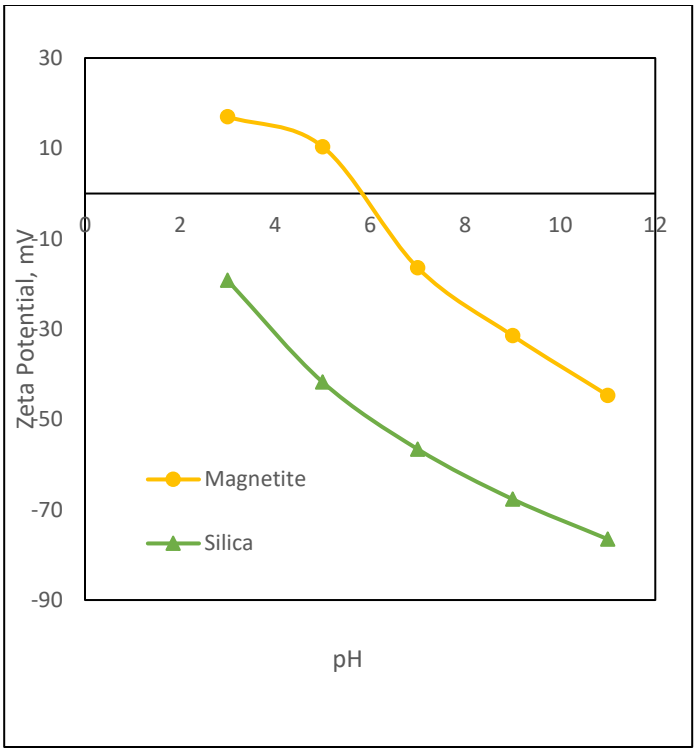

Figure 5. Zeta Potential of Magnetite and Silica at 0.001M KNO_3

The experimentally determined Hamaker constant for magnetite and the Hamaker constant for silica obtained from literature, $2.5x10^{-21}$ J, as reported in the study made by Watillon et al.[31], and the zeta potential values obtained in Figure 5 are used to construct the total potential energy curves.

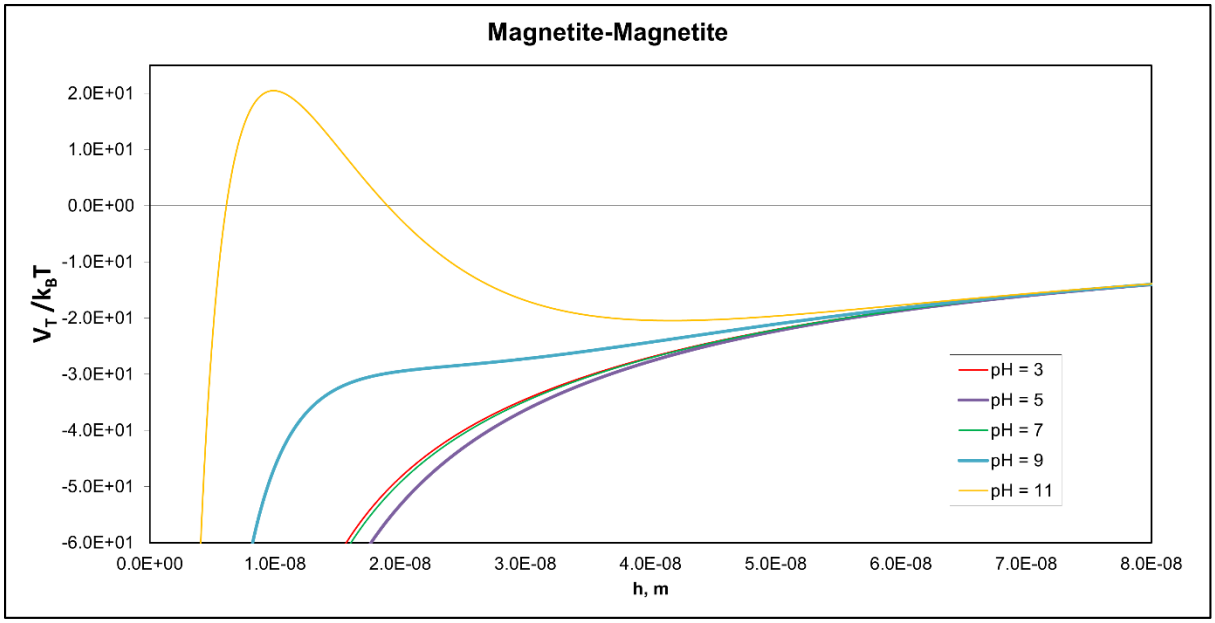

Figure 6. Potential energy curve of the magnetite-magnetite system at different pH values with k_b = 1.38 x 10^{-23} J K^{-1} (Boltzmann constant) and T = 298.15 K (temperature).

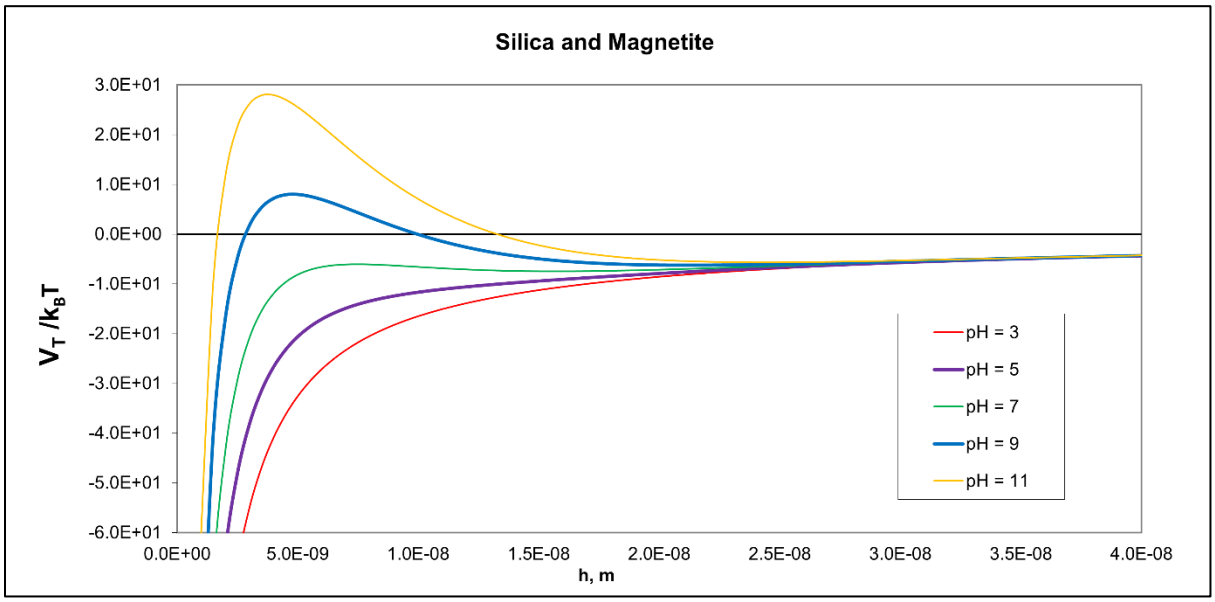

Figure 7. Potential energy curve of the silica-magnetite system at different pH values with k_b = 1.38 x 10-23 J K-1 (Boltzmann constant) and T = 298.15 K (temperature).

3.1.2. DLVO Calculation

The total interaction energy V_T for the interaction of magnetite particles at different pH values is shown in Figure 6. The zeta potential values of magnetite in Figure 5 and the experimentally determined Hamaker constant for magnetite were used in Equations 2 and 3 to generate the V_T curve for magnetite-magnetite interactions.

The potential energy curves shown in Figure 6 for magnetite-magnetite interactions indicate that the energy barrier for attraction is low at pH 3-9. Based on this, increased aggregation of magnetite particles should be observed at pH 3-9. The increased aggregation causes the magnetite particles to settle faster at these pH levels, thus, increasing the likelihood of the particles to be retained during enhanced gravity concentration. [12] Meanwhile, at pH 11, Figure 6 indicates a higher energy barrier which favors repulsion. At pH 11, wherein repulsion is dominant, the magnetite particles settle slower, thus, increasing the likelihood of the particles reporting to the overflow stream. [8][11][12]

The V_T of magnetite-silica particles at different pH values is also shown in Figure 7. The zeta potential values of magnetite and silica in Figure 5, the experimentally determined Hamaker constant for magnetite, and the Hamaker constant for silica were used in Equations 4 and 5 to generate the V_T curves for magnetite-silica interactions.

As shown in the potential energy curve in Figure 7, the smallest energy barrier needed for attraction was found at pH 3, 5 and 7. Due to this small energy barrier which favors the formation of more aggregates of silica and magnetite, settling rate was faster. As seen in Figure 5, the zeta potential of magnetite at pH 3, 5 and 7 is positive and the zeta potential of silica is negative. The difference in polarity of the charges at these conditions increases the probability for attraction to occur. [36] The potential energy curve also shows that a high energy barrier must be overcome for attraction to occur at pH 9 and 11. The results obtained agree with the findings of Dobryden et al., which also reported repulsive interactions between magnetite and silica at pH $\geq$ 9, and attractive interactions below pH 8.[36] The zeta potential of both silica and magnetite at pH 9 and 11 are both negative which increases the probability of repulsion to occur. [36]

The particle interactions of silica and magnetite can also affect the likelihood of recovering magnetite during enhanced gravity concentration. The enhanced settling rate of magnetite and silica also at pH 3, 5 and 7 is expected to increase the probability of the particles reporting to the retention zone. [11][12] The presence of silica, however, might lower the separation efficiency of the enhanced gravity concentration.

3.2 Enhanced Gravity Concentration at Different Electrostatic Conditions

The performance of the enhanced gravity concentration in terms of recovery and separation efficiency as a function of suspension pH is shown in Figure 8. The recovery of magnetite and silica was computed by taking the weight of the mineral recovered and dividing it by the total weight of the mineral in the feed. Separation efficiency was computed by subtracting the recovery of gangue R_g in the concentrate from the recovery of the valuable mineral R_m as shown in the equation 5.[1]

$$\text{Separation Efficiency (SE)} = R_m - R_g \quad \textbf{(7)}$$

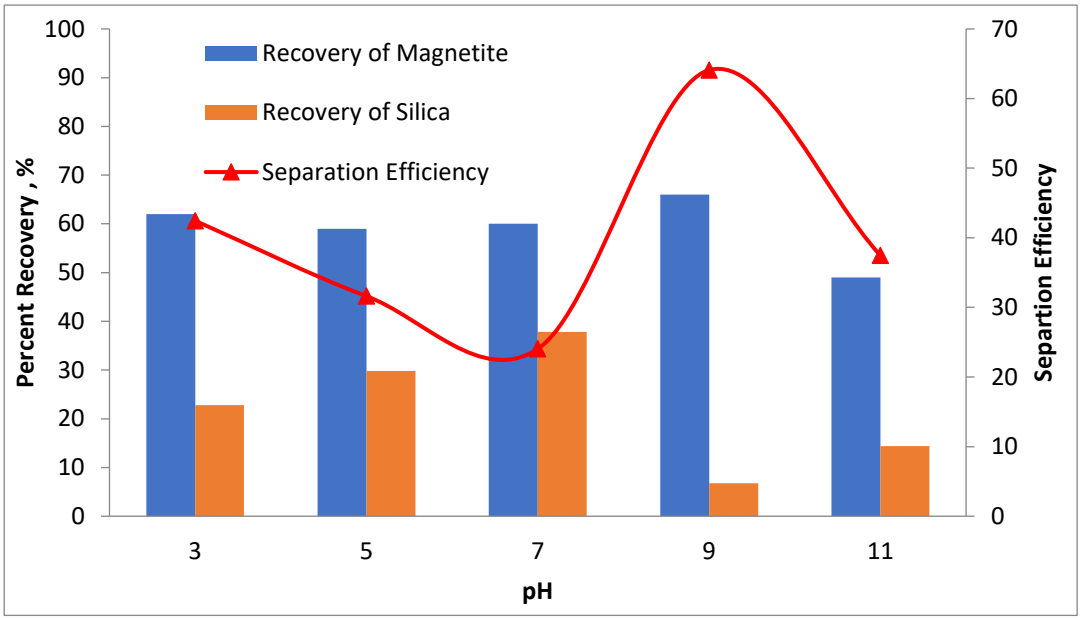

Figure 8. Recovery and Separation Efficiency of magnetite and silica at different pH levels

Figure 8 indicates that the recovery of magnetite is higher at pH 3-9 wherein attractive forces are dominant for the magnetite-magnetite interactions. The recoveries obtained in all conditions are close to 60%, with the highest magnetite recovery of 66% occurring at pH 9. Increased agglomeration at these conditions allows the magnetite particles to have a faster settling rate. [26] These magnetite particles would report to the walls of the concentrate bowl and be retained. [12][6] The lowest magnetite recovery was found at pH 11 at just 49%. At this pH, repulsive forces are dominant as shown in the potential energy curve in Figure 6. The weaker interaction between magnetite particles at this condition decreases their settling rates and, consequently, the probability for recovery. [12][6]

The increased recovery of magnetite at pH 3, 5 and 7 can also be attributed to the interaction of magnetite and silica particles as shown in Figure 7. The potential energy curves at these pH values indicate an attractive interaction between magnetite and silica, which favors faster settling of the two minerals. The faster settling rate also increases the likelihood of both minerals being retained within the concentrate bowl. Since both magnetite and silica report to the concentrate, decreased separation efficiency was observed, as shown in Figure 8.

Similar to the interaction of magnetite-magnetite particles at pH 11, the dominant interaction of magnetite-silica particles was also repulsion at this condition, as presented in Figure 7. The repulsive interaction of magnetite and silica further decreases the probability to form agglomerates that increase settling rate. Recoveries of both minerals were observed to be relatively low at this condition.

The highest separation efficiency was observed at pH 9 as presented in Figure 8. At this condition, the potential energy curves show that the interaction between magnetite particles was attraction while the magnetite-silica interaction was repulsion. The repulsive interaction between magnetite and silica decreased the probability of silica being included in the concentrate. The higher magnetite recovery at this condition can also be attributed to the increased repulsive interaction between magnetite and silica particles since fewer entrained magnetite particles join the silica particles reporting to the tailings. Since magnetite recovery is high and silica recovery is low, the separation is more efficient at this condition.

IV. CONCLUSIONS

The study used classical DLVO theory to determine the effect of electrostatic interactions in the separation of magnetite and silica particles subjected to the Falcon concentrator. To construct the total potential energy graphs in the DLVO analysis, an experimentally obtained Hamaker constant for magnetite was determined to be 2.22×10^{-20} J. The potential energy curves generated for the magnetite-magnetite interactions showed that attractive forces were dominant at pH 3-9, and repulsive forces at pH 11. For magnetite-silica interactions, the potential energy curves generated showed that attraction was the dominant interaction at pH 3-7 and repulsion at pH 9 and 11. The results of the enhanced gravity concentration experiments agree with the predicted results of the DLVO analysis, showing increased recovery of magnetite at pH 3-7 where attractive forces are dominant for magnetite-magnetite interactions. The attractive interaction between magnetite-silica, however, resulted in a decrease in separation efficiency as more silica particles were entrained with the concentrate. The highest separation efficiency of 64.1% was found at pH 9 which was the only condition where magnetite-silica interactions were repulsive, and magnetite-magnetite interactions were attractive.

V. RECOMMENDATIONS

The emphasis on future work on the effect of electrostatic interactions on Falcon gravity concentration should focus on using actual ore samples. The investigation would be more complex since more mineral interactions need to be accounted for. The potential impact on the operation of enhanced gravity concentration, however, would be even greater. It is also recommended that a study be made using the smooth bowl which does not have a provision for fluidization. The separation on this type of bowl would be controlled mainly by the rotational speed of the Falcon concentrator and the characteristics of the feed material.

VI. ACKNOWLEDGEMENTS

The equipment used in this study were procured through the ERDT-BetterMine Project of the University of the Philippines and the Department of Science and Technology.

REFERENCES

[1] Wills BA, Barry A, Napier-Munn T, 2006. Wills' mineral processing technology: an introduction to the practical aspects of ore treatment and mineral recovery. Elsevier/BH.

[2] Turner JF. 1991. Gravity concentration, past, present and future. Minerals Engineering. 4(3–4):213–223.

[3] Burt R. 1999. The role of gravity concentration in modern processing plants. Mineral Engineering. 12:1291–1300.

[4] Honaker RQ. 1998. High capacity fine coal cleaning using an enhanced gravity concentrator. Mineral Engineering. 11:1191–1199.

[5] Laplante AR. 1993. A comparative study of two centrifugal concentrators-annotated. Canadian Mineral Processors Proceedings.

[6] Farajzadeh S, Chehreh Chelgani S. 2022. Gravity separation by concentrator- an over review. Separation Science and Technology. Philadelphia. 00(00):1–20. https://doi.org/10.1080/01496395.2022.2028836. doi:10.1080/01496395.2022.2028836

[7] Dehaine Q, Foucaud Y, Kroll-Rabotin JS, Filippov LO. 2019. Experimental investigation into the kinetics of Falcon UF concentration: Implications for fluid dynamic-based modelling. Separation and Purification Technology. 215:590–601. https://doi.org/10.1016/j.seppur.2019.01.048. doi:10.1016/j.seppur.2019.01.048

[8] Kroll-Rabotin JS, Bourgeois F, Climent É. 2012. Experimental validation of a fluid dynamics based model of the UF Falcon concentrator in the ultrafine range. Separation and Purification Technology. 92:129–135. doi:10.1016/j.seppur.2011.10.029

[9] Honaker RQ, Wang D, Hot K. 1996. Application of the Falcon Concentrator for fine coal cleaning.

[10] Kroll-Rabotin JS, Bourgeois F, Climent É. 2009. Fluid dynamics based modelling of the Falcon concentrator for ultrafine particle beneficiation. Minerals Engineering. 23(4):313–320. doi:10.1016/j.mineng.2009.10.001

[11] Kroll-Rabotin JS, Bourgeois F, Climent É. 2013. Physical analysis and modeling of the Falcon concentrator for beneficiation of ultrafine particles. International Journal of Mineral Processing. 121:39–50. doi:10.1016/j.minpro.2013.02.009

[12] Galvin KP, Dickinson JE. 2013. Particle transport and separation in inclined channels subject to centrifugal forces. Chemical Engineering Science. 87:294–305. doi:10.1016/j.ces.2012.10.023

[13] Marion C, Langlois R, Kökkılıç O, Zhou M, Williams H, Awais M, Rowson NA, Waters KE. 2019. A design of experiments investigation into the processing of fine low specific gravity minerals using a laboratory Knelson Concentrator. Minerals Engineering. 135:139–155. doi:10.1016/j.mineng.2018.08.023

[14] Van Hee P, Lin WK, Benac-Vegas L, Van der Lans RGJM, Koper GJM, Van der Wielen LAM. 2006. Selective recovery of micrometer particles from mixtures using a combination of selective aggregation and dissolved-air flotation. Colloids and Surfaces A: Physicochemical and Engineering Aspects. 280(1–3):216–231. doi:10.1016/j.colsurfa.2006.02.003

[15] Li D, Yin W, Liu Q, Cao S, Sun Q, Zhao C, Yao J. 2017. Interactions between fine and coarse hematite particles in aqueous suspension and their implications for flotation. Minerals Engineering. 114:74–81. http://dx.doi.org/10.1016/j.mineng.2017.09.012. doi:10.1016/j.mineng.2017.09.012

[16] Vergouw JM, Difeo A, Xu Z, Finch JA. 1998. An agglomeration study of sulphide minerals using zeta potential and settling rate. Part II: Sphalerite/pyrite and sphalerite/galena. Minerals Engineering. 11(7):605–614. doi:10.1016/s0892-6875(98)00045-4

[17] Ramos-Tejada MM, Ontiveros A, Viota JL, Durán JDG. 2003. Interfacial and rheological properties of humic acid/hematite suspensions. Journal of Colloid and Interface Science. 268(1):85–95. doi:10.1016/S0021-9797(03)00665-9

[18] Oruç F, Özgen S, Sabah E. 2010. An enhanced-gravity method to recover ultra-fine coal from tailings: Falcon concentrator. Fuel. 89(9):2433–2437. doi:10.1016/j.fuel.2010.04.009

[19] Holtham PN. 1992. Particle transport in gravity concentrators and the Bagnold effect.

[20] Hartmann R, Kinnunen P, Illikainen M. 2018. Cellulose-mineral interactions based on the DLVO theory and their correlation with flotability. Minerals Engineering. 122:44–52. https://doi.org/10.1016/j.mineng.2018.03.023. doi:10.1016/j.mineng.2018.03.023

[21] Sun Z, Liu J, Xu S. 2006. Study on improving the turbidity measurement of the absolute coagulation rate constant. Langmuir. 22(11):4946–4951. doi:10.1021/la0602160

[22] Chheda P, Grasso D, van Oss CJ. 1992. Impact of ozone on stability of montmorillonite suspensions. Journal of Colloid and Interface Science. 153(1):226–236. doi:10.1016/0021-9797(92)90314-C

[23] Boylu F. 2013. Modeling of free and hindered settling conditions for fine coal beneficiation through a falcon concentrator. International Journal of Coal Preparation and Utilization. 33(6):277–289. doi:10.1080/19392699.2013.818986

[24] Derjaguin B, Landau L. 1993. Theory of the stability of strongly charged lyophobic sols and of the adhesion of strongly charged particles in solutions of electrolytes. Progress in Surface Science. 43(1–4):30–59. doi:10.1016/0079-6816(93)90013-L

[25] Verwey EJW, Laboratorium N, Waals D. Theory stability. 1946:631–636.

[26] Hu JD, Zevi Y, Kou XM, Xiao J, Wang XJ, Jin Y. 2010. Effect of dissolved organic matter on the stability of magnetite nanoparticles under different pH and ionic strength conditions. Science of the Total Environment. 408(16):3477–3489. http://dx.doi.org/10.1016/j.scitotenv.2010.03.033. doi:10.1016/j.scitotenv.2010.03.033

[27] Harding RD. 1972. Heterocoagulation in mixed dispersions-effect of particle size, size ratio, relative concentration, and surface potential of colloidal components. Journal of Colloid And Interface Science. 40(2):164–173. doi:10.1016/0021-9797(72)90006-9

[28] Hogg R, Healy TW, Fuerstenau DW. 1966. Mutual coagulation of colloidal dispersions. Transactions of the Faraday Society. 62(615):1638–1651. doi:10.1039/tf9666201638

[29] García-García S, Wold S, Jonsson M. 2007. Kinetic determination of critical coagulation concentrations for sodium- and calcium-montmorillonite colloids in NaCl and CaCl2 aqueous solutions. Journal of Colloid and Interface Science. 315(2):512–519. doi:10.1016/j.jcis.2007.07.002

[30] Mosley LM, Hunter KA, Ducker WA. 2003. Forces between colloid particles in natural waters. Environmental Science and Technology. 37(15):3303–3308. doi:10.1021/es026216d

[31] Depasse J, Watillon A. 1970. The Stability of Amorphous Colloidal Silica. Journal of Colloid and Interface Science. 33:430–438.

[32] Ackler HD, French RH, Chiang YM. 1996. Comparisons of Hamaker constants for ceramic systems with intervening vacuum or water: From force laws and physical properties. Journal of Colloid and Interface Science. 179(2):460–469. doi:10.1006/jcis.1996.0238

[33] Liu J, Dai C, Hu Y. 2018. Aqueous aggregation behavior of citric acid coated magnetite nanoparticles: Effects of pH, cations, anions, and humic acid. Environmental Research. 161:49–60. doi:10.1016/j.envres.2017.10.045

[34] Chen KL, Elimelech M. 2007. Influence of humic acid on the aggregation kinetics of fullerene (C60) nanoparticles in monovalent and divalent electrolyte solutions. Journal of Colloid and Interface Science. 309(1):126–134. doi:10.1016/j.jcis.2007.01.074

[35] Faure B, Salazar-Alvarez G, Bergström L. 2011. Hamaker constants of iron oxide nanoparticles. Langmuir. 27(14):8659–8664. doi:10.1021/la201387d

[36] Dobryden I, Mensi E, Holmgren A, Almqvist N. 2020. Surface forces between nanomagnetite and silica in aqueous ca2+ solutions studied with afm colloidal probe method. Journal of Colloids and Interfaces. 4(3). doi:10.3390/colloids4030041